Chiang Mai J. Sci. 2010; 37(2) : 252-259
www.science.cmu.ac.th/journal-science/josci.html
Contributed Paper

Monte Carlo Investigation of Ferromagnetic Properties Under Compressive Stress

Yongyut Laosiritaworn*[a,b], Supon Ananta [a] and Rattikorn Yimnirun [c]

[a] Department of Physics and Materials Science, Faculty of Science, Chiang Mai University, Chiang Mai 50200, Thailand.

[b] ThEP Center, CHE, 328 Si Ayutthaya Road, Bangkok 10400, Thailand.

[c] School of Physics, Institute of Science, Suranaree University of Technology, Nakhon Ratchasima 30000, Thailand.

*Author for correspondence; e-mail: yongyut_laosiritaworn@yahoo.com

Received: 11 December 2009
Accepted: 19 January 2010

ABSTRACT

In this work, we used Monte Carlo simulations to model the three-dimensional ferromagnetic Ising spins under the influence of uniaxial and hydrostatic compressive mechanical stresses. The study was performed with a cluster-flip algorithm to investigate how the magnetic properties including critical behaviors depend on temperatures and the applied mechanical stresses. From the results, the magnetic profiles as a function of temperature were obtained and it was found that the applied stresses lowered the magnetic phase transition point. However, the critical exponents to the relevant observables did not significantly change. This suggests universality behavior in magnetic systems under loading environment.

Keywords: Ising model, Monte Carlo, compressive mechanical stress, magnetic properties.

1. INTRODUCTION

Ferromagnetic materials have long been of interest in view of both technological and fundamental importance [1-3] especially in magnetic recording where high areal densities are in demand [1]. Therefore, it is necessary to understand ferromagnetic behavior in details. Nevertheless, real magnetic materials used in many applications are often affected from stress, while the study can not be trivially taken due to the structural complexity. Even without external stress, e.g. in thin-films, the stress can be induced by different lattice spacing at the interfaces between ferromagnetic layers and the substrate leading to strong magnetic anisotropy [4-6] and fascinating magnetic behavior. For instance, magnetic systems under stresses were found to have substantial changes in magnetic phases and their transition [7-9]. In addition, the anti-ferromagnet behavior can be removed or promoted [7-10]. Furthermore, the critical temperature was found to change by varying the magnitude of stresses [11-17]. However, theoretical investigations usually considered the stress in terms of lattice distortion which alters the magnetic interaction among spins [17,19], whereas the direct effect of the stress type and magnitude on magnetic properties

is still left to identify. Therefore, it is the objective of this study to model such a situation to provide a better understanding of magnetic materials under loading environment.

2. METHODOLOGIES

In this study, we considered the Ising Hamiltonian

$$H = \sum_{<ij>} J_{ij}\left(r_{ij}\right) s_i s_j \qquad (1)$$

where the spin $s_i = \pm 1$ and $<ij>$ indicates the sum includes only nearest neighboring pairs. The exchange interaction $J_{ij}(r_{ij})$ is a function of lattice spacing r_{ij} between sites i and j. Since J_{ij} has its origin from the exchanged electron wave functions, it should change with changing the lattice spacing. Therefore, J_{ij} is assumed to take a Lennard-Jones potential like i.e. [17,19]

$$J_{ij}\left(r_{ij}\right) = J_0\left[\left(\frac{r_0}{r_{ij}}\right)^{12} - 2\left(\frac{r_0}{r_{ij}}\right)^{6}\right], \qquad (2)$$

where r_0 is the stress-free lattice spacing, and J_0 is the ferromagnetic exchange interaction associated with r_0. For zero stress (strain), $r_{ij} = r_0$ and $J_{ij} = -J_0$ which prefers ferromagnetic phase. Since the Young's modulus is defined as $Y \equiv \sigma/[(r_{ij} - r_0)/r_0]$ [20] and if the stress σ is in the z direction, it is possible to write $r_{ij}^z / r_0 = 1+\sigma/Y$ so $J_{ij} = J_{ij}^z = J_0\left[(1+\sigma/Y)^{-12} - 2(1+\sigma/Y)^{-6}\right]$. Note that $\sigma/Y < 0$ is for compressive stress which is the considered case in this study.

However, if the stress is uniaxial type, there occur lattice distortions for both z direction (contraction) and the $x(y)$ direction (expansion). The ratio of these distortions is defined as the Poisson ratio

$$\varepsilon \equiv -\frac{\Delta r^{x(y)}}{\Delta r^{z}} = -\frac{r_{ij}^{x(y)} - r_0}{r_{ij}^{z} - r_0} = \frac{1 - r_{ij}^{x(y)}/r_0}{r_{ij}^{z}/r_0 - 1}$$

(where in many materials, $\varepsilon \approx 0.3$ [20]). Therefore, $r_{ij}^{xy}/r_0 = 1-\varepsilon\left(r_{ij}^{z}/r_0 - 1\right) = 1-\varepsilon\sigma/Y$. Consequently, along the $x(y)$ direction, $J_{ij} = J_{ij}^{xy} = J_0\left[\left(1-\varepsilon\sigma/Y\right)^{-12} - 2\left(1-\varepsilon\sigma/Y\right)^{-6}\right]$. Accordingly, the Hamiltonian under the effect of the uniaxial stress can be written as

$$H = \sum_{<ij>\in xy} J_{ij}^{xy} s_i s_j + \sum_{<ij>\in z} J_{ij}^{z} s_i s_j. \qquad (3)$$

On a contrary, for the hydrostatic type, the stress is applied to all directions. Therefore, in cubic structure, the lattice spacing reduces in size with a same magnitude for all x, y and z directions. Consequently, all nearest neighboring spins interact with a same J_{ij}^{z} so equation (3) still applies but one has to note $J_{ij}^{xy} = J_{ij}^{z}$.

Nevertheless, from equation (2), J_{ij} becomes anti-ferromagnetic preference at large stress i.e. $J_{ij}^{z} > 0$ for $(1+\sigma/Y)^{-12} > 2(1+\sigma/Y)^{-6}$. Therefore, if $\sigma/Y < \sqrt[6]{1/2} - 1 \approx -0.109$, the spins will prefer anti-ferromagnetic coupling. However, $\sigma \ll Y$ should be considered in modeling the material in its elastic range [20]. Therefore, we considered the compressive stress in the range $-0.10 \le \sigma/Y \le 0.00$ where ferromagnetic preference is guaranteed. Note that the Young's modulus varies from materials to materials, so there is a benefit in specifying the stress in terms of σ/Y ratio instead of the bare σ.

Throughout this study, J_0 was set to 1 so this defined the unit of J_0/k_B for temperatures (where k_B is the Boltzmann's constant). Note that by setting J_0 as the energy unit, the results obtained from this work can be applied to model any 3D Ising-like magnetic materials. Specifically, in modeling a particular material, J_0 of that material (in real energy unit which can be calculated from electronic structure calculations), is required to covert the units of other parameters into appropriate units. For instance, to convert the critical temperature T_C from J_0/k_B unit to Kelvin unit can be done by direct substitution of J_0, while there is no need to repeat the simulation. In addition,

one may use $J_{ij} = +J_0$ instead of $J_{ij} = -J_0$ in modeling general anti-ferromagnetic materials.

In this work, the simulations were done on simple cubic lattices with a total number of spins $N = L^3$, where L ranges from 20 to 60, and periodic boundary is used. The temperatures T was varied from 2.0 to 5.0 J_0/k_B, and σ/Y is varied from -0.10 to 0.00. Unit time was defined from one full update of all spins i.e. 1 mcs. The spin configurations were updated using the Wolff algorithm [21] to minimize correlation time and statistical errors [22], where clusters of spins were formed with a probability

$$p = 1 - \exp\left\{\min\left(0, -\frac{2J_{ij}s_i s_j}{k_B T}\right)\right\} \quad (4)$$

and flipped. Both uniaxial and hydrostatic stresses were considered. For the uniaxial stress, $\varepsilon = 0.3$ was used, and $J_{ij} = J_{ij}^{xy}$ was set if spins couple in the $x(y)$ direction, but $J_{ij} = J_{ij}^{z}$ was set for the applied stress direction (z direction). Nonetheless, $J_{ij} = J_{ij}^{z}$ for all coupling directions for the hydrostatic stress.

In each simulation, after equilibration, the magnetization and the energy were measured with an interval about 1 mcs. N' (=5,000) different configurations were used to calculate the magnetization $\langle m \rangle = (1/N')\sum_t^{N'} |m_t|$ (where $m_t = (1/N)\Sigma_i s_i(t)$) as well as the magnetic susceptibility $\chi = (N/k_B T)\left(\langle m^2 \rangle - \langle m \rangle^2\right)$. After that, via the fourth order cumulant $U_L = 1 - \langle m^4 \rangle / 3\langle m^2 \rangle^2$ [23] and the single histogram method [24], the critical temperature T_C was extracted by measuring the temperatures $T_C(b=L/L')$ from cumulant crossing for differing sized L and L' and extrapolating $T_C(b)$ to the limit $(\ln b)^{-1} \to 0$ [22,23]. In addition, based on the finite-size scaling ansatz, the scaling forms of how m and χ scale with L were considered i.e. [25,26]

$$\langle m(T) \rangle = L^{-\beta/\nu} \tilde{m}\left(L^{1/\nu} t\right), \quad (5)$$

$$\chi(T) = L^{\gamma/\nu} \tilde{\chi}\left(L^{1/\nu} t\right), \quad (6)$$

where γ, β, and ν are the critical exponents associated with χ, m, and the correlation length ξ, respectively. $\tilde{\chi}$ and $\tilde{m}$ are scaling functions and $t = T/T_C - 1$. These scaling functions for a range of L should collapse onto a single curve with correct critical temperature and critical exponents, so β/ν and γ/ν can be extracted from the slopes of the log-log plots of m or χ against L at T_C. Similarly, $1/\nu$ can be extracted from cumulant derivative since $dU_L/d(k_B T) \propto L^{1/\nu}$ at T_C [23]. Furthermore, based on the hyperscaling relation [27], it is possible to extract the system dimensionality $d = 2\beta/\nu + \gamma/\nu$, where $d = 3$ is expected for three-dimensional (3D) behavior.

3. RESULTS AND DISCUSSION

The magnetization and magnetic susceptibility profiles are presented in Figure 1, where the phase transition point is found to shift to lower temperatures with increasing stresses. This is since the increase of stresses reduces the exchange interaction and hence the energy. Therefore, the compressed system does not require as much the thermal energy (and temperature) as the uncompressed system to go from ferromagnetic to paramagnetic phase. The results for critical temperatures and exponents are presented in Table 1 for both uniaxial and hydrostatic stresses, where the graphical representations are shown in Figures (2,3). Notice that the hydrostatic stress provides lower critical points than the uniaxial stress at a same magnitude since the uniaxial has larger exchange interaction in the $x(y)$

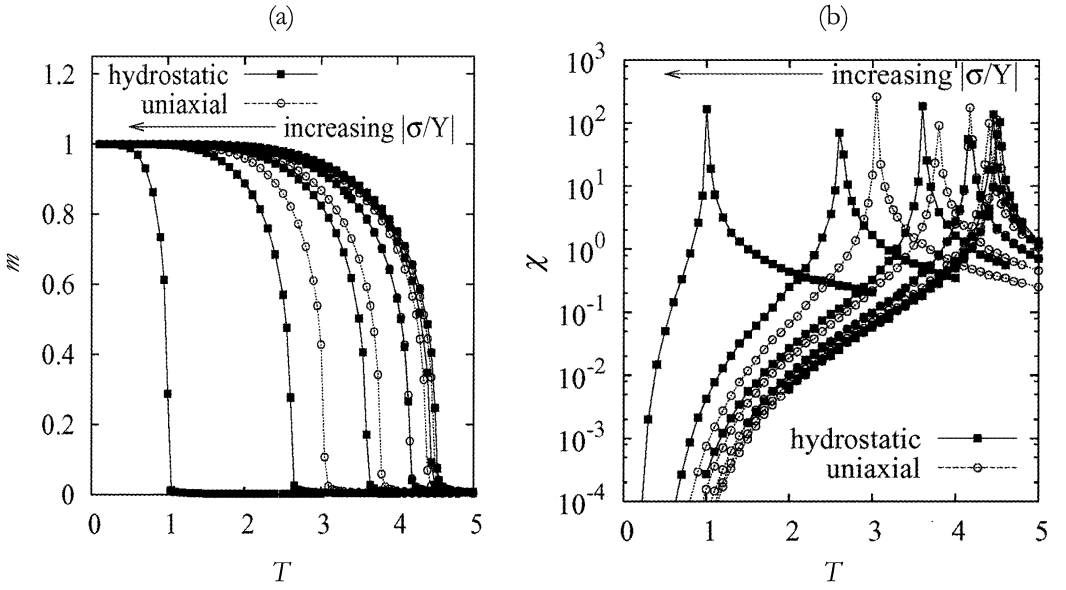

Figure 1. The magnetic properties of 3D Ising spins with N = 60 x 60 x 60 spins under uniaxial and hydrostatic compressive stresses from Monte Carlo simulations. From right to left, for each type of the stress, the stress magnitude increases from $|\sigma/Y|$ = 0.00 to 0.10 in steps of 0.02. A shift of phase transition point to lower temperatures with increase magnitude of stresses is evident for (a) m and (b) χ respectively. Lines are used for viewing aids.

Table 1. Critical temperatures T_C, the critical exponents (β/ν,γ/ν,$1/\nu$) and the dimension d obtained from Monte Carlo simulation for uniaxial and hydrostatic compressive stresses.

Stress type	σ/Y	T_C	β/ν	γ/ν	$1/\nu$	$d=2\beta/\nu+\gamma/\nu$
N/A	0.00	4.5121±0.0003	0.509±0.005	1.958±0.007	1.522±0.017	2.976±0.016
uniaxial	-0.02	4.4833±0.0004	0.507±0.004	1.956±0.008	1.514±0.021	2.969±0.015
	-0.04	4.3805±0.0002	0.505±0.004	1.960±0.007	1.514±0.015	2.969±0.015
	-0.06	4.1680±0.0003	0.505±0.002	1.958±0.008	1.524±0.018	2.968±0.012
	-0.08	3.7794±0.0003	0.499±0.004	1.956±0.006	1.515±0.015	2.955±0.014
	-0.10	3.0437±0.0002	0.504±0.004	1.959±0.004	1.545±0.014	2.966±0.013
Hydro-static	-0.02	4.4371±0.0002	0.510±0.004	1.972±0.006	1.560±0.009	2.993±0.013
	-0.04	4.1645±0.0002	0.508±0.003	1.960±0.004	1.535±0.014	2.976±0.009
	-0.06	3.6002±0.0003	0.507±0.004	1.968±0.007	1.524±0.013	2.983±0.014
	-0.08	2.6104±0.0002	0.508±0.003	1.968±0.009	1.542±0.021	2.985±0.016
	-0.10	1.0046±0.0001	0.505±0.003	1.966±0.006	1.523±0.017	2.976±0.011

direction. However, both stresses show that T_C reduces with increasing the stresses while the stress-free results agree well with previous Monte Carlo investigations on 3D Ising spins [25]. Note that the reduction in T_C with increasing stresses agrees with references [11,12,15,16] but disagrees with references [13,14,17]. This could be caused by that, in

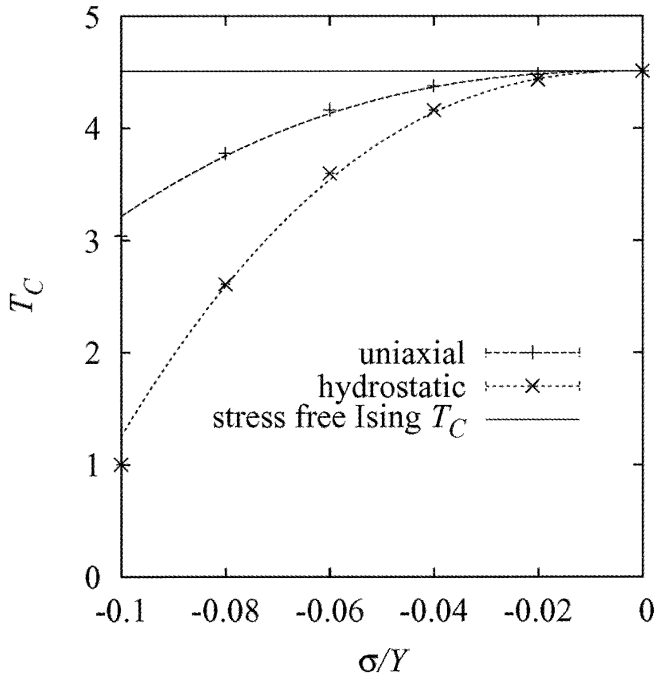

Figure 2. The critical temperatures T_C as a function of stresses extracted from Monte Carlo simulations. The zero stress results agree well with previous studies [25]. The curves are drawn from non-linear fits to the data i.e. equation (7).

addition to the exchange interaction, the stress may induce some shape (directional) anisotropies which change the ground state and increase the system Hamiltonian [10]. Therefore, to investigate the increase of T_C with stresses, material and structural dependence on stresses of the anisotropies should be also considered.

However, as can be seen in Figure 2, T_C tends to relate to σ/Y in a power law form i.e.

$$T_C\left(\frac{\sigma}{Y}\right) = T_C(0) - a \times \left|\frac{\sigma}{Y}\right|^b, \qquad (7)$$

where $T_C(0)$ refers to stress-free critical temperature, and a and b are constants. Therefore, if the relation as in equation (7) can be formulated, the knowledge on how the critical temperature associates to the stress will be revealed. Nevertheless, a straightforward non-linear fit does not function since only a small number of data is available. Fortunately, as the stress-free $T_C(0)$ was known (see Table 1), equation (7) may change to

$$\log\left(T_C(0) - T_C\left(\frac{\sigma}{Y}\right)\right) = \log a - b \log\left|\frac{\sigma}{Y}\right|, \qquad (8)$$

where a and b can be extracted from the linear fit of the log-log plot of equation (8). With the proposed fit, the uniaxial stress gives a = 336.1139 ± 88.4584 and b = 2.4137 ± 0.0875 with R^2 = 0.99804, while the hydrostatic stress gives a= 776.6502 ± 132.2325 and b = 2.3771 ± 0.0566 with R^2 = 0.99915. As a result, with the known constants (a,b), equation (7) can be used to draw non-linear relation between T_C and σ/Y as is in Figure 2. The curves seem to match up with the data except at the highest σ/Y = -0.10 since the error in a is quite large. Furthermore, it can be seen the both type of stresses appear to agree in the value of b within error bars. This suggests that the type of stress may not affect the universality of how the

magnitude of stresses alters the critical temperature.

Next, on further verifying the contention of universality, the critical exponents were considered since they have been known to depend only on the system dimension and the order parameter, but not on the magnitude and range of the interaction [28]. Consequently, the exponents (β/ν, γ/ν and $1/\nu$) were extracted from the slopes of the log-log plots of m, χ and $dU_L/d(k_BT)$ against L at T_C (according to equations (5,6) and that $dU_L/d(k_BT) \propto L^{1/\nu}$. Good linear relations were found from all log-log plots (not shown) which support the validity of finite size scaling ansatz for magnetic systems under stresses. These exponents including the dimension $d = 2\beta/\nu+\gamma/\nu$ are graphically presented in Figure 3, where both types of stresses agree on the values. Again, the stress-free results are

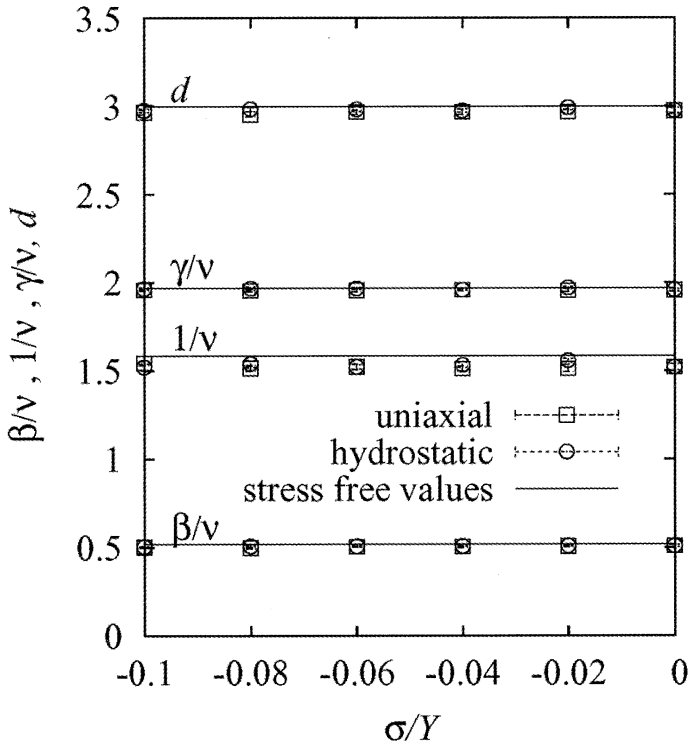

Figure 3. Critical exponents ($1/\nu$,β/ν, and γ/ν) and the dimension d for both uniaxial and hydrostatic compressive stresses. Linear horizontal lines are the values from previous stress-free investigation [25].

in consistent with the previous investigation [25] (straight lines). As being evident, types and magnitude of stresses (as long as the system is of the same type e.g. ferromagnetic) do not affect the universality of the magnetic systems. Furthermore, as the dimension d is close to 3, this implies that three-dimensional magnetic behavior is not affected by the structure deformation.

4. CONCLUSIONS

To conclude, this study proposes Monte Carlo simulations to study the three-dimensional Ising spins under the influence of

uniaxial and hydrostatic stresses via the Lennard-Jones type exchange interaction to observe magnetic properties. The critical temperature is found to reduce with increasing the stress magnitude. However, the critical exponents and the hyperscaling dimension do not change with types and magnitude of the stresses which secure the contention of magnetic universality in compressed magnetic systems.

ACKNOWLEDGEMENTS

This work was supported by the Industry/University Cooperative Research Center (I/UCRC) in HDD Component, the Faculty of Engineering, Khon Kaen University and National Electronics and Computer Technology Center, National Science and Technology Development Agency.

REFERENCES

[1] Judy J.H., Past, Present, and Future of Perpendicular Magnetic Recording, *J. Magn. Magn. Mater.*, 2001; **235:** 235-240.

[2] Moser A., Takano K., Margulies D.T., Albrecht M., Sonobe Y., Ikeda Y., Sun S. and Fullerton E.E., Magnetic Recording: Advancing into the Future, *J. Phys. D*, 2002; **35:** R157-R167.

[3] Spaldin N.A., *Magnetic Materials: Fundamentals and Device Applications*, Cambridge University Press, Cambridge, 2003.

[4] O'Brien W.L. and Tonner B.P., Transition to the Perpendicular Easy Axis of Magnetization in Ni Ultrathin Films Found by X-Ray Magnetic Circular Dichroism, *Phys. Rev. B*, 1994; **49:** 15370-15373.

[5] Sander D., Enders A. and Kirschner J., Stress and Magnetic Properties of Surfaces and Ultrathin Films, *J. Magn. Magn. Mater.*, 1999; **200**: 439-455.

[6] Wulfhekel W., Zavaliche F., Porrati F., Oepen H.P. and Kirschner J., Nano-Patterning of Magnetic Anisotropy by Controlled Strain Relief, *Europhys. Lett.*, 2000; **49**: 651-657.

[7] Gu L., Chakraborty B., Garrido P.L., Phani M. and Lebowitz J.L., Monte Carlo Study of a Compressible Ising Antiferromagnet on a Triangular Lattice, *Phys. Rev. B*, 1996; **53:** 11985-11992.

[8] Andrianov A.Vl., Bauer E., Paul Ch. and Savel'eva O.A., Pressure-Induced Helical Antiferromagnetism in Ferromagnetic $Ho_{40}Gd_{60}$, *J. Magn. Magn. Mater.*, 2004; **272–276:** E451-E452.

[9] Sushko Y.V., DeHarak B., Cao G., Shaw G., Powell D.K. and Brill J.W., Hydrostatic Pressure Effects on the Magnetic Susceptibility of Ruthenium Oxide $Sr_3Ru_2O_7$: Evidence for Pressure-Enhanced Antiferromagnetic Instability, *Solid State Commun.*, 2004; **130:** 341-346.

[10] Murata T., Kushida H., Terai T. and Kakeshita T., Pressure-Induced Magnetic Transition of Layered Manganite $La_{2-2x}Sr_{1+2x}Mn_2O_7$ (x=0.315, 0.318), *J. Magn. Magn. Mater.*, 2007; **310:** 1555-1557.

[11] Burghardt T., Hallmann E. and Eichler A., Breakdown of Ferromagnetism in $CePd_2Ga_3$ under High Pressure, *Physica B*, 1997; **230-232**: 214-216.

[12] Looney C.W., Falk K., Hamlin J.J., Tomita T., Schilling J.S., Haase W. and Tomkowicz Z., Hydrostatic Pressure Dependence of the Curie Temperature of [MnR_4TPP] [TCNE] for R=$OC_{10}H_{21}$, $OC_{14}H_{29}$, and F (TPP, tetraphenylporhyrin; TCNE, tetracyanoethylene), *Polyhedron*, 2003; **22:** 3339-3344.

[13] Nicklas M., Moreno N.O., Borges H.A., Bauer E.D., Sarrao J.L. and Thompson J.D., Effect of Pressure on the Ferromagnetic Compound $CeCu_2Ga_2$, *J. Magn. Magn. Mater.*, 2004; **272-276:** E111-E112.

[14] Arumugam S., Mydeen K., Fontes M., Manivannan N., Vanji M.K., RamaTulasi K.U., Ramos S.M., Saitovitch E.B., Prabhakaran D. and Boothroyd A.T., Effect of Pressure and Magnetic Field on Bilayer $La_{1.25}Sr_{1.75}Mn_2O_7$ Single Crystal, *Solid State Commun.*, 2005; **136:** 292-296.

[15] Sidorov V.A., Rakhmanina A.V. and Morya O.A., Influence of High Pressure on the Ferromagnetic Transition Temperature of CrO_2, *Solid State Commun.*, 2006; **139:** 360-362.

[16] Hamasaki T., Kuroe H., Sekine T., Naka T., Hase M., Maeshima N., Saiga Y. and Uwatoko Y., Effects of High Pressure on $A_2Cu_2Mo_3O_{12}$ (A=Rb,Cs): A One-Dimensional System with Competing Ferromagnetic and Antiferromagnetic Interactions, *J. Magn. Magn. Mater.*, 2007; **310**: E394-E396.

[17] Markovich V., Fita I., Puzniak R., Martin C., Wisniewski A., Yaicle C., Maignan A., and Gorodetsky G., Pressure Effect on Magnetism in Phase-Separated Cr-Doped $Pr_{0.5}Ca_{0.5}Mn_{1-x}Cr_xO_3$ Manganites, *J. Magn. Magn. Mater.*, 2007; **316:** E636-E639.

[18] Boubcheur E.H. and Diep H.T., Effect of Elastic Interaction on Critical Behavior of Three-Dimensional Ising Model, *J. Appl. Phys.*, 1999; **85:** 6085-6087; Ngo V.T. and Diep H.T., Monte Carlo Study of Surface-Frustrated Heisenberg Thin Films with Magnetoelastic Coupling: An Off-Lattice Model , *J. Appl. Phys.*, 2002; **91:** 8399.

[19] Mitchell S.J. and Landau D.P., Phase Separation in a Compressible 2D Ising Model, *Phys. Rev. Lett.*, 2006; **97:** 025701.

[20] Callister W.D., *Materials Science and Engineering: An Introduction*, John Wiley and Sons, New York, 2003.

[21] Wolff U., Collective Monte Carlo Updating for Spin Systems, *Phys. Rev. Lett.*, 1989; **62:** 361-364.

[22] Binder K. and Heermann D.W., *Monte Carlo Simulation in Statistical Physics*, Springer–Verlag, Berlin, 1992.

[23] Binder K., Finite Size Scaling Analysis of Ising Model Block Distribution Functions, *Z. Phys. B*, 1981; **43:** 119-140.

[24] Ferrenberg A.M. and Swendsen R.H., New Monte Carlo Technique for Studying Phase Transitions, *Phys. Rev. Lett.*, 1988; **61**: 2635-2638.

[25] Ferrenberg A.M. and Landau D.P., Critical Behavior of the Three-Dimensional Ising Model: A High-Resolution Monte Carlo Study, *Phys. Rev. B*, 1991; **44**: 5081-5091.

[26] Newman M.E.J. and Barkema G.T., *Monte Carlo Methods in Statistical Physics*, Oxford University Press, New York, 1999.

[27] Fisher M.E., Rigorous Inequalities for Critical-Point Correlation Exponents, *Phys. Rev.*, 1969; **180:** 594-600.

[28] Stanley H.E., Scaling, Universality, and Renormalization: Three Pillars of Modern Critical Phenomena, *Rev. Mod. Phys.*, 1999; **71:** S358-S366 *and references therein.*